



THE UNIVERSITY *of* EDINBURGH

Edinburgh Research Explorer

A Physical Model of the Prepared Piano

Citation for published version:

Ducceschi, M & Bilbao, S 2019, A Physical Model of the Prepared Piano. in *Proceedings of the 26th International Congress on Sound and Vibration*. Canadian Acoustical Association, Montreal.

Link:

[Link to publication record in Edinburgh Research Explorer](#)

Document Version:

Publisher's PDF, also known as Version of record

Published In:

Proceedings of the 26th International Congress on Sound and Vibration

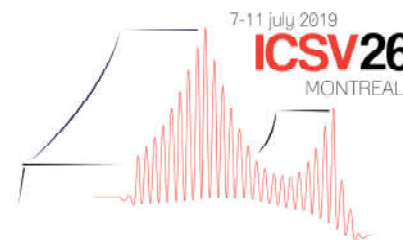
General rights

Copyright for the publications made accessible via the Edinburgh Research Explorer is retained by the author(s) and / or other copyright owners and it is a condition of accessing these publications that users recognise and abide by the legal requirements associated with these rights.

Take down policy

The University of Edinburgh has made every reasonable effort to ensure that Edinburgh Research Explorer content complies with UK legislation. If you believe that the public display of this file breaches copyright please contact openaccess@ed.ac.uk providing details, and we will remove access to the work immediately and investigate your claim.





A PHYSICAL MODEL FOR THE PREPARED PIANO

Michele Ducceschi, Stefan Bilbao

University of Edinburgh, UK

email: michele.ducceschi@ed.ac.uk

This work presents a model of a prepared piano, suitable for sound synthesis purposes. The strings, acting as primary resonators, are modelled in some detail, including geometric nonlinear effects, and the string-hammer interaction is also included. The resonating body, the soundboard, is assumed to be of rectangular shape. Virtual microphones are placed across the soundboard and along the strings. Moreover, the strings can be prepared by means of objects such as nails and dampers. This model is intended to be a useful and efficient tool for synthesising piano sounds, with extensive control over the instrument design.

Keywords: physical modelling, finite difference schemes, modal methods, piano acoustics, musical acoustics

1. Introduction

Piano modelling represents a topic of longstanding interest in musical acoustics and digital sound synthesis. Various models, with varying degrees of refinement, have been proposed in the literature. Of notable interest are the works of Giordano [1], of Bank et al. [2], and of Chabassier et al. [3]. In the current work, a realistic, efficient model of a piano is implemented for sound synthesis purposes. The model can be tuned by choosing a number of physical parameters for the strings, the soundboard and the hammers. Moreover, various elements such as nails, dampers, and rattles, can be added to the system, in order to “prepare” the piano (see [4]). The complete system presents numerous nonlinearities: these are in the form of distributed geometrical nonlinearities in the strings themselves, and in the form of collision forces arising during contact of the strings with the hammers and with the preparation elements. Remarkably, the whole system can be solved by a simple matrix inversion at each time step. Stability may be inferred by energy arguments, both for the distributed nonlinearities (see [5, 6]), and for the lumped collisions. The latter, in particular, are simulated via a suitable quadratisation of the nonlinear collision potentials, and this is an element of novelty with respect to previous works. Quadratisation of nonlinearities has been employed in the context of virtual-analog modelling (see [7, 8, 9]), and has recently been extended by these authors to partial differential equations of interest in musical acoustics [10, 11].

2. Continuous Model

In this section, the continuous equations for the prepared piano are presented. The piano is composed of a set of strings, attached to a soundboard via a bridge. Strings are set into motion by hammers, and

preparation elements act on the strings.

2.1 Strings

In piano strings two model features lead to prominent perceptual effects: stiffness, and geometric nonlinearities. The former can be modelled via an appropriate engineering beam model. In previous works (see, e.g. [3]), refined models including rotational vibrations of the cross section, as per the Timoshenko model, have been used. This choice is motivated by the relatively large thickness of the low-pitched piano strings. Surprisingly, even for such strings, stiffness effects can be faithfully reproduced by means of simpler models (such as Euler-Bernoulli [12]), which will be employed here. Nonlinearities in piano strings, giving rise to important perceptual phenomena such as phantom partials, arise at high vibration amplitudes. These geometrical effects can be modelled by a convenient power series expansion, as per the model of Morse and Ingard [6]. A system of partial differential equations including all of the above features may be written as

$$\mathcal{L}_s w_s = \frac{E_s A_s - T_s}{2} \partial_{x_s} [(\partial_{x_s} w_s)^3 + 2(\partial_{x_s} w_s)(\partial_{x_s} \zeta_s)] + \sum_{p=1}^{P_s} \delta^{(1)}(x_s - x_{(s,p)}) B_{(s,p)} + \delta^{(1)}(x_s - x_{(s,b)}) F_s^w \quad (1a)$$

$$\mathcal{G}_s \zeta_s = \frac{E_s A_s - T_s}{2} \partial_{x_s} [(\partial_{x_s} w_s)^2] + \delta^{(1)}(x_s - x_{(s,b)}) F_s^\zeta \quad (1b)$$

Above, the symbols $\mathcal{L}_s, \mathcal{G}_s$ are linear differential operators given by

$$\begin{aligned} \mathcal{L}_s &= \rho_s A_s \partial_t^2 - T_s \partial_{x_s}^2 + E_s I_s \partial_{x_s}^4 + 2\rho_s A_s \sigma_s^{(w)} \partial_t - 2\rho_s A_s \tau_s^{(w)} \partial_t \partial_{x_s}^2 \\ \mathcal{G}_s &= \rho_s A_s \partial_t^2 - E_s A_s \partial_{x_s}^2 + 2\rho_s A_s \sigma_s^{(\zeta)} \partial_t \end{aligned}$$

In the equations, the transverse and longitudinal displacements are given as $w_s(t, x_s)$ and $\zeta_s(t, x_s)$, respectively. The piano has a total number of S strings, and the index s denotes the s^{th} string. The domain of definition of the string is $x_s \in \mathcal{D}_s = [0, L_s]$, where L_s is the length of the unstretched string. The symbols $\partial_t, \partial_{x_s}$ indicate partial derivatives along t, x_s respectively. Constants appear as: ρ_s , the volumetric density; A_s , the area of the cross section; T_s , the applied tension; E_s , Young's modulus. Loss coefficients are given as $\sigma_s^{(w)}, \sigma_s^{(\zeta)}, \tau_s^{(w)}$, with the first two being measured in s^{-1} , and the latter being measured in $m^2 s^{-1}$, hence resulting in a wavenumber-dependent loss. The symbols $\delta^{(1)}$ represent one-dimensional Dirac deltas. The symbol $B_{(s,p)}$ represents a forcing term (measured in Newtons) coming from the point-wise contact of the string with the p^{th} lumped object (i.e. the mallet, or a preparation element). It is assumed that a total number P_s of such lumped objects is acting on the s^{th} string at any given time, at the locations $x_{(s,p)}$. Expressions for the $B_{(s,p)}$ terms are detailed in 2.4. Finally, F_s^w, F_s^ζ are the forces exerted by the bridge on the strings. The bridge is located at $x_{(s,b)}$, and expressions for such forces are given in 2.3.

In view of the energy analysis in Section 3, an inner product and associated norm are given here as

$$\langle a, b \rangle_{\mathcal{D}_s} \triangleq \int_0^{L_s} ab \, dx_s, \quad \|a\|_{\mathcal{D}_s} \triangleq \sqrt{\langle a, a \rangle_{\mathcal{D}_s}}, \quad (2)$$

where a, b are two well-behaved functions defined over \mathcal{D}_s .

2.2 Soundboard

Soundboards in pianos are complex engineering systems, whose complete modelling requires a considerable effort [13]. Alternatively, one may record an impulse response from which the modal properties

of the soundboard may be extracted [2]. In this work, a simplified model of the soundboard is offered, so as to allow design flexibility, yet maintaining a simple form that can be solved with an efficient modal approach (see Section 4.2). Similarly to the case of strings, the thickness of the soundboard is such that higher-order effects induced by the rotations of the cross section can be safely neglected [14], and hence one may introduce an appropriate model via the orthotropic Kirchhoff plate equations. In Cartesian coordinates, these are

$$(\rho_p H \partial_t^2 - T_p (\partial_X^2 + \partial_Y^2) + 2\rho_p H \chi \partial_t + [\partial_X^2, \partial_Y^2] \mathbf{D} [\partial_X^2, \partial_Y^2]^T) W = - \sum_{s=1}^S \delta^{(2)}(\mathbf{X} - \mathbf{X}_{(s)}) (F_s^w + F_s^\zeta) \quad (3)$$

where the rigidity matrix is defined as

$$\mathbf{D} \triangleq \begin{bmatrix} D_X & D_{XY} \\ D_{XY} & D_Y \end{bmatrix} = \begin{bmatrix} (E_X H^3)/(12(1 - \nu_X \nu_Y)) & D_X \nu_Y + (GH^3)/6 \\ D_X \nu_Y + (GH^3)/6 & (E_Y H^3)/(12(1 - \nu_X \nu_Y)) \end{bmatrix}$$

The flexural displacement of the plate is denoted by $W = W(t, \mathbf{X})$. The plate occupies a rectangular portion of space, so $\mathbf{X} \triangleq (X, Y) \in \mathcal{A} = [0, L_X] \times [0, L_Y]$, with L_X, L_Y being the side lengths. Partial derivatives along X, Y are denoted by ∂_X, ∂_Y . Constants appear as: ρ_p , the volumetric density; T_p , the applied tension at the boundaries; H the thickness of the plate; χ is a loss factor; E_X, E_Y are the Young's moduli in the orthogonal X and Y directions; ν_X and ν_Y are the Poisson's ratios, and G is the modulus of rigidity. On the right hand side, the symbol $\delta^{(2)}(\mathbf{X} - \mathbf{X}_{(s)})$ is a two-dimensional Dirac delta. Each of the string is attached to the plate at the location specified by $\mathbf{X}_{(s)}$. (Do not mistake the string coordinate x_s for the location on the soundboard of the bridge connection of the s^{th} string $\mathbf{X}_{(s)}$.) The symbols F_s^w, F_s^ζ represent the forcing terms (measured in Newtons) transmitted from the strings via the bridge, as per (1a), (1b). Similarly to the case of strings, an inner product and associated norm can be defined on the domain of the plate, in the following manner

$$\langle f, g \rangle_{\mathcal{A}} \triangleq \int_0^{L_X} \int_0^{L_Y} f g \, dX \, dY \quad \|f\|_{\mathcal{A}} \triangleq \sqrt{\langle f, f \rangle_{\mathcal{A}}} \quad (4)$$

2.3 Bridge

The bridge is here simply modelled as a combination of linear springs. Each string is connected at one of its point to the plate, via two linear springs, one for the transverse, and one for the longitudinal direction, and both inducing a flexural force in the plate, as per (3). In theory, one should set up the bridge connection at one of the string ends. However, in the discretisation of the string equations given in 4.1, the resulting discrete expressions for the boundary forces present several nonlinear terms, which may pose a problem when setting the ghost points so to guarantee passivity of the termination. In practice, one may attach the bridge at an interior point, very close to the string end, and work with fixed boundary conditions. In any case, the forces F_s, R_s appearing in (1a), (1b), (3) are

$$F_s^w = -K_s^w \Delta_s^w \triangleq -K_s^w (w_s(t, x_{(s,b)}) - W(t, \mathbf{X}_{(s)})) \quad (5a)$$

$$F_s^\zeta = -K_s^\zeta \Delta_s^\zeta \triangleq -K_s^\zeta (\zeta_s(t, x_{(s,b)}) - W(t, \mathbf{X}_{(s)})) \quad (5b)$$

where K_s^w, K_s^ζ are the transverse and longitudinal elastic constants of the springs of the s^{th} string.

2.4 Hammers and Preparation Elements

Piano hammers are known to play an important role in the production of sound. Realistic sound synthesis may be realised by considering an appropriate single-sided power law: this model has been

successfully employed to describe collisions in musical acoustics [15]. The interaction force between a lumped object and one string may be given as

$$B_{(s,p)} = d\phi_{(s,p)}/d\eta_{(s,p)} + \beta_{(s,p)}\dot{\eta}_{(s,p)} \quad \text{with} \quad \eta_{(s,p)} = U_{(s,p)}(t) - w(t, x_{(s,p)}), \quad (6)$$

In the above, $\phi_{(s,p)}$ represents a potential, depending on $\eta_{(s,p)}$, which is the length characterising the amount of compression of the string and the lumped object in contact; $U_{(s,p)}$ is the displacement of the lumped object, colliding with the string at the location $x_{(s,p)}$; $\beta_{(s,p)} \geq 0$ is a loss factor. A second equation is needed, to describe the motion of the lumped object. This is

$$M_{(s,p)}\ddot{U}_{(s,p)} = -B_{(s,p)} \quad (7)$$

Various forms of the potential can be given. For hammers, a particularly useful one is

$$\phi(\eta_{(s,p)}) = \frac{G_{(s,p)}}{\alpha_{(s,p)} + 1} [\eta_{(s,p)}]_+^{\alpha_{(s,p)}+1} \quad \text{with} \quad [\eta_{(s,p)}]_+ \triangleq 0.5(\eta_{(s,p)} + |\eta_{(s,p)}|) \quad (8)$$

In the above, $G_{(s,p)}$ is a stiffness constant; $\alpha_{(s,p)} \geq 1$ is an exponent characterising the collision. The symbol $[x]_+$ denotes the positive part of x , which is nonzero only if $x > 0$: this definition is useful to characterise single-sided forces.

Preparation elements such as rattles are characterised by a length $\epsilon_{(s,p)}$, and the potential is

$$\phi(\eta_{(s,p)}) = \frac{G_{(s,p)}}{\alpha_{(s,p)} + 1} [|\eta_{(s,p)}| - \epsilon_{(s,p)}]_+^{\alpha_{(s,p)}+1} \quad (9)$$

In this case, a force will be exerted if $|\eta_{(s,p)}| > \epsilon_{(s,p)}$, resulting in intermittent contact between the string and the rattle, and generating nonlinear forces. For lack of space, more complex preparation elements will not be discussed here. These include nonlinear string coupling devices, dampers, etc. See [4, 11].

3. Conservation of Energy of the Continuous Model

In the absence of all dissipation, the prepared piano model described above is conservative. In the remainder, the indices (s) , (p) , (b) , (t) will denote, respectively, the string, the hammer and preparation elements, the bridge and the soundboard. Double indices such as (s, p) and (s, b) will denote terms involving the string plus the hammer/preparation elements and bridge. Now, perform the following steps in order to obtain an energy balance for the complete system

- Take an inner product of the form (2) of $\partial_t w_s$ with (1a), $\forall s$
- Take an inner product of the form (2) of $\partial_t \zeta_s$ with (1b), $\forall s$
- Take an inner product of the form (4) of $\partial_t W$ with (3)
- Multiply (7) by $\dot{U}_{(s,h)}$
- Sum up the scalar equations resulting from steps (a)-(d)

After convenient integration by parts (not shown here for lack of space), one obtains the following energy balance

$$\frac{d}{dt}\mathcal{H} = 0 \quad \text{where} \quad \mathcal{H} = \sum_{s=1}^S \left(\mathcal{H}_k^{(s)} + \mathcal{H}_{pl}^{(s)} + \mathcal{H}_{pnl}^{(s)} + \mathcal{H}_{pl}^{(s,b)} + \sum_{p=1}^{P_s} \left(\mathcal{H}_{coll}^{(s,p)} + \mathcal{H}_k^{(s,p)} \right) \right) + \mathcal{H}_k^{(t)} + \mathcal{H}_{pl}^{(t)} \quad (10)$$

The total energy is written as a sum of various components: the index k denotes a kinetic component, the index pl denotes a potential giving rise to a linear force, the index pnl denotes a potential giving rise to a nonlinear force, and the index $coll$ denotes the collision potential. The analytic expressions are

$$\begin{aligned}
 \mathcal{H}_k^{(s)} &= \frac{\rho_s A_s}{2} \|\partial_t w_s\|_{\mathcal{D}_s}^2 + \frac{\rho_s A_s}{2} \|\partial_t \zeta_s\|_{\mathcal{D}_s}^2 & \mathcal{H}_{pl}^{(t)} &= \frac{D_x}{2} \|\partial_x^2 W\|_{\mathcal{A}}^2 + \frac{D_y}{2} \|\partial_y^2 W\|_{\mathcal{A}}^2 + D_{xy} \|\partial_y \partial_x W\|_{\mathcal{A}}^2 \\
 \mathcal{H}_{pl}^{(s)} &= \frac{T_s}{2} \|\partial_{x_s} w_s\|_{\mathcal{D}_s}^2 + \frac{E_s I_s}{2} \|\partial_{x_s}^2 w_s\|_{\mathcal{D}_s}^2 + \frac{T_s}{2} \|\partial_{x_s} \zeta_s\|_{\mathcal{D}_s}^2 & \mathcal{H}_k^{(s,p)} &= \frac{M_{(s,p)}}{2} (\dot{U}_{(s,p)})^2 \\
 \mathcal{H}_{pnl}^{(s)} &= \frac{E_s A_s - T_s}{2} \left\| \frac{(\partial_{x_s} w_s)^2}{2} + \partial_{x_s} \zeta_s \right\|_{\mathcal{D}_s}^2 & \mathcal{H}_{coll}^{(s,p)} &= \phi(\eta_{(s,p)}) \\
 \mathcal{H}_k^{(t)} &= \frac{\rho_p H}{2} \|\partial_t W\|_{\mathcal{A}}^2 & \mathcal{H}_{pl}^{(s,b)} &= \frac{K_s^w}{2} (\Delta_s^w)^2 + \frac{K_s^\zeta}{2} (\Delta_s^\zeta)^2
 \end{aligned}$$

where $\phi(\eta_{(s,p)})$ is as per (8), (9), and where $\Delta_s^w, \Delta_s^\zeta$ are as per (5a), (5b). The total energy is non-negative if $E_s A_s \geq T_s$ which is the case for musical strings, and under a suitable choice of boundary conditions. These are chosen as

$$w_s(t, 0) = \zeta_s(t, 0) = w_s(t, L_s) = \zeta_s(t, L_s) = \partial_x^2 w_s(t, 0) = \partial_x^2 w_s(t, L_s) = 0 \quad \forall s \quad (11a)$$

$$W = \partial_n^2 W = 0 \text{ along the boundary of the plate; } n \text{ is the direction normal to the boundary} \quad (11b)$$

Non-negativity results in boundedness of the norms of the displacements and their derivatives.

4. Discrete Model

In this section, a suitable discretisation of the full system is given. The discrete model will be written as a hybrid finite difference/modal method, for which suitable stability conditions will be extracted after an energy analysis.

4.1 Strings

The strings are simulated via the finite difference method. The continuous functions $w_s(t, x_s)$, $\zeta_s(t, x_s)$ are approximated by grid functions $w_s^{n,m} \triangleq w_s(nk, mh_s)$, $\zeta_s^{n,m} \triangleq \zeta_s(nk, mh_s)$, where the indices m, n are positive integers, and where k is the time step, and h_s is the grid spacing of the s^{th} string. It is assumed that $n \geq 0$ and $0 \leq m \leq M_s$, and thus the grid spacing h_s divides the domain L_s in M_s equal intervals. Finite difference operators are now introduced. The identity and time shifting operators are

$$1w_s^{n,m} = w_s^{n,m}, \quad e_{t+}w_s^{n,m} = w_s^{n+1,m}, \quad e_{t-}w_s^{n,m} = w_s^{n-1,m} \quad (12)$$

From those, the time difference operators are introduced as

$$\delta_{t+} \triangleq \frac{e_{t+} - 1}{k}, \quad \delta_{t-} \triangleq \frac{1 - e_{t-}}{k}, \quad \delta_{t\cdot} \triangleq \frac{e_{t+} - e_{t-}}{2k}, \quad \delta_{tt} \triangleq \delta_{t+}\delta_{t-} \quad (13)$$

Time averaging operators are

$$\mu_{t+}\mu_{t-} \triangleq \frac{1 + e_{t+}}{2}, \quad \mu_{t-} \triangleq \frac{1 + e_{t-}}{2}, \quad \mu_{t\cdot} \triangleq \frac{e_{t+} + e_{t-}}{2}, \quad \mu_{tt} \triangleq \mu_{t+}\mu_{t-} \quad (14)$$

Space shifting operators are defined as

$$e_{x+}^s w_s^{n,m} = w_s^{n,m+1}, \quad e_{x-}^s w_s^{n,m} = w_s^{n,m-1} \quad (15)$$

From those, space difference operators are given as

$$\delta_{x+}^s \triangleq \frac{e_{x+}^s - 1}{h_s}, \quad \delta_{x-}^s \triangleq \frac{1 - e_{x-}^s}{h_s}, \quad \delta_{x\cdot}^s \triangleq \frac{e_{x+}^s - e_{x-}^s}{2h_s}, \quad \delta_{xx}^s \triangleq \delta_{x+}^s \delta_{x-}^s, \quad \delta_{xxx}^s \triangleq \delta_{xx}^s \delta_{x\cdot}^s \quad (16)$$

Given the definitions $v_s \triangleq \delta_{x-}^s w_s^{n,m}$, $z_s \triangleq \delta_{x-}^s \zeta_s^{n,m}$ (1) is discretised as

$$(\rho_s A_s \delta_{tt} - T_s \delta_{xx}^s + E_s I_s \delta_{xxxx}^s + 2\rho_s A_s \sigma_s^{(w)} \delta_t - 2\rho_s A_s \tau_s^{(w)} \delta_t \delta_{xx}^s) w_s^{n,m} = \frac{E_s A_s - T_s}{2} \delta_{x+}^s [(v_s)^2 (\mu_t v_s) + 2(v)(\mu_{tt} z_s)] + \sum_{p=1}^{P_s} \mathcal{I}_p(x_{(s,p)}) b_{(s,p)} + \mathcal{I}_b(x_{(s,b)}) f_s^w \quad (17a)$$

$$(\rho_s A_s \delta_{tt} - E_s A_s \delta_{xx}^s \mu_{tt} + 2\rho_s A_s \sigma_s^{(\zeta)} \delta_t) \zeta_s^{n,m} = \frac{E_s A_s - T_s}{2} \delta_{x+}^s [(v_s)(\mu_t v_s)] + \mathcal{I}_b(x_{(s,b)}) f_s^\zeta \quad (17b)$$

where

$$\mathcal{I}_o(x_{(s,o)}) = \begin{cases} 1/h_s, & m = m_o = \text{round}(x_{(s,o)}/h_s) \\ 0, & \text{otherwise} \end{cases}$$

and where $b_{(s,p)}$, f_s^w , f_s^ζ are discrete versions of, respectively, the collision forces $B_{(s,p)}$, and of the bridge forces F_s^w , F_s^ζ , and given below in 4.3, 4.4.

4.2 Soundboard

Vibrations of the soundboard will be calculated using a modal approach. Thanks to this approach, it is possible to set the decay times mode by mode, thus giving the user extensive control on reverberation. The modal equations are independent, hence yielding a natural parallel structure which can be easily optimised numerically. Moreover, convenient modal pruning strategies can be devised to improve efficiency even further [16]. Hence

$$W(t, \mathbf{X}) = \sum_{r_X=1}^{R_X} \sum_{r_Y=1}^{R_Y} q_{r_X, r_Y}(t) s_{r_X}(X) s_{r_Y}(Y) \quad \text{where } s_{r_X}(X) s_{r_Y}(Y) \triangleq \sin \frac{r_X \pi X}{L_X} \sin \frac{r_Y \pi Y}{L_Y}, \quad (r_X, r_Y) \in \mathbb{N}$$

Using this expression, which satisfies the boundary conditions (11b), in (3), and projecting onto one mode by means of the scalar product (4), one gets the modal equation

$$\ddot{q}_{r_X, r_Y} + \Omega_{r_X, r_Y}^2 q_{r_X, r_Y} + 2\chi_{r_X, r_Y} \dot{q}_{r_X, r_Y} = - \sum_{s=1}^S \frac{4s_{r_X}(X_s) s_{r_Y}(Y_s)}{L_X L_Y \rho_p H} (F_s^w + F_s^\zeta) \quad (18)$$

where the loss coefficients χ are now mode-dependent. The modal frequencies are

$$\Omega_{r_X, r_Y}^2 = \frac{T_p}{\rho_p H} \left[\frac{r_X^2 \pi^2}{L_X^2} + \frac{r_Y^2 \pi^2}{L_Y^2} \right] + \frac{D_X r_X^4 \pi^4}{\rho_p H L_X^4} + \frac{D_Y r_Y^4 \pi^4}{\rho_p H L_Y^4} + \frac{2D_{XY} r_X^2 r_Y^2 \pi^4}{\rho_p H L_X^2 L_Y^2} \quad (19)$$

A numerical scheme for (18) is obtained immediately after the substitution of the continuous functions $\ddot{q}_{r_X, r_Y}(t)$ and $\dot{q}_{r_X, r_Y}(t)$ with their discrete counterparts $\delta_{tt} q_{r_X, r_Y}^n$, $\delta_t q_{r_X, r_Y}^n$, and where the continuous bridge forces F_s^w , F_s^ζ are replaced by f_s^w , f_s^ζ , given below.

4.3 Bridge

A discretisation of the continuous bridge forces is obtained immediately as

$$f_s^w = -K_s^w \left(w_s^{n, m_b} - \sum_{r_X, r_Y} q_{r_X, r_Y}^n s_{r_X}(X_s) s_{r_Y}(Y_s) \right) \quad (20a)$$

$$f_s^\zeta = -K_s^\zeta \left(\zeta_s^{n, m_b} - \sum_{r_X, r_Y} q_{r_X, r_Y}^n s_{r_X}(X_s) s_{r_Y}(Y_s) \right) \quad (20b)$$

where m_b is the index corresponding to the bridge location along the string.

4.4 Hammers and Preparation Elements

The schemes for the hammers and for the preparation elements will be derived here by means of energy-conserving finite-difference schemes, following a convenient quadratisation of the nonlinear collision potential yielding, ultimately, a form of the update which does not require an iterative solver (e.g. Newton-Raphson.) For details, see [10, 11]. This numerical aspect represents an element of novelty of the current work. Upon the introduction of an auxiliary function $\psi_{(s,p)}$, the hammer force $B_{(s,p)}$ is approximated by the discrete force $b_{(s,p)}$ given by

$$\begin{cases} b_{(s,p)} &= g^n \left(\mu_{t+} \psi_{(s,p)}^{n-1/2} \right) \\ \delta_{t+} \psi_{(s,p)}^{n-1/2} &= g^n \left(\delta_t \eta_{(s,p)}^n \right) \end{cases} \quad (21) \quad \text{where} \quad g^n = \frac{\partial \psi_{(s,p)}}{\partial \eta_{(s,p)}} \Big|_{\eta_{(s,p)} = \eta_{(s,p)}^n}$$

Above, g^n is calculated as the analytic derivative of the function $\psi \triangleq \sqrt{2\phi}$, and ϕ is as per (8), (9).

5. Conservation of Energy of the Discrete Model

The particular discretisation given here is conservative. The energy components, discrete counterparts of (10), are not given here for lack of space. However, conditions for the non-negativity of the energy function as a whole are given. First, a set of numerical boundary conditions, consistent with (11a), is given here as

$$w_s^{n,0} = \zeta_s^{n,0} = w_s^{n,M_s} = \zeta_s^{n,M_s} = \delta_{xx}^s w_s^{m,0} = \delta_{xx}^s w_s^{n,M_s} = 0 \quad (22)$$

Three conditions must be imposed, $\forall s$:

$$\rho_s A_s h_s^4 - K_s^w k^2 h_s^3 - T_s k^2 h_s^2 - 4E_s I_s k^2 \geq 0 \quad (23a)$$

$$K_s^\zeta < \frac{\rho_s A_s h_s}{k^2} \quad (23b)$$

$$\frac{\Omega_{rX,rY}^2}{4} + \frac{4R \max(K_s^w, K_s^\zeta)}{L_x L_y \rho_p H} < \frac{1}{k^2} \quad (23c)$$

The first inequality must be solved via an iterative solver such as Newton-Raphson. The second inequality gives an upper bound on the choice of the longitudinal stiffness constant, while the last inequality poses an upper bound on the largest eigenfrequency of the soundboard (R being the total number of modes). If the three conditions above are satisfied, the discrete energy is guaranteed to be non-negative at all times. Non-negativity of the discrete energy allows to bound the norms of the grid functions, and hence stability of the numerical scheme follows.

6. Numerical Experiments and Sound Examples

Sound examples of the prepared piano are presented in the companion web page of this paper, at the address <http://mdphys.org/preparedpiano.html>

7. Acknowledgments

The first author wishes to thank the Leverhulme Trust, who is supporting his research with an Early Career Fellowship.

References

1. Giordano, N. Finite difference modeling of the piano, *J. Acoust. Soc. Am.*, **119** (5), 3291–3291, (2006).
2. Bank, B., Zambon, S. and Fontana, F. A modal-based real-time piano synthesizer, *IEEE/ACM Trans. Audio, Speech, Language Process.*, **18** (4), 809–821, (2010).
3. Chabassier, J., Chaigne, A. and Joly, P. Modeling and simulation of a grand piano, *J. Acoust. Soc. Am.*, **134** (1), 648–665, (2013).
4. Bilbao, S. and Ffitch, J. Prepared piano sound synthesis, *Proc. Int. Conf. On Dig. Audio Eff. (DAFx 2006)*, Montreal, Canada, September, (2006).
5. Bilbao, S. Conservative numerical methods for nonlinear strings, *J. Acoust. Soc. Am.*, **118**, 3316–3327, (2005).
6. Bilbao, S., *Numerical Sound Synthesis: Finite Difference Schemes and Simulation in Musical Acoustics*, Wiley, Chichester, UK (2009).
7. Lopes, N., Hélie, T. and Falaize, A. Explicit second-order accurate method for the passive guaranteed simulation of port-hamiltonian systems, *Proc. 5th IFAC 2015*, Lyon, France, July, (2015).
8. Falaize, A. and Hélie, T. Passive Guaranteed Simulation of Analog Audio Circuits: A Port-Hamiltonian Approach, *Appl. Sci.*, **6**, 273 – 273, (2016).
9. Falaize, A., *Modélisation, simulation, génération de code et correction de systèmes multi-physiques audios: Approche par réseau de composants et formulation Hamiltonienne À Ports*, Ph.D. thesis, Université Pierre et Marie Curie, Paris, (2016).
10. Ducceschi, M. and Bilbao, S., (2019), *Non-iterative Solvers for Nonlinear Problems: The Case Of Collisions*. Under review, 22nd Int. Conf. on Dig. Audio Eff. (DAFx 2019).
11. Bilbao, S., Ducceschi, M. and Webb, C., (2019), *A Large-scale real-time Modular Physical Modeling Sound Synthesis System*. Under review, 22nd Int. Conf. on Dig. Audio Eff. (DAFx 2019).
12. Ducceschi, M. and Bilbao, S. Linear stiff string vibrations in musical acoustics: Assessment and comparison of models, *J. Acoust. Soc. Am.*, **140** (4), 2445–2454, (2016).
13. Chaigne, A., Cotte, B. and Viggiano, R. Dynamical properties of piano soundboards, *J. Acoust. Soc. Am.*, **133** (4), 2456–2466, (2013).
14. Torin, A., *Percussion Instrument Modelling In 3D: Sound Synthesis Through Time Domain Numerical Simulation*, Ph.D. thesis, University of Edinburgh, Edinburgh, UK, (2015).
15. Bilbao, S., Torin, A. and Chatziioannou, V. Numerical modeling of collisions in musical instruments, *Acta Acust. United Ac.*, **101**, 155 – 173, (2015).
16. Ducceschi, M. and Webb, C. Plate reverberation: Towards the development of a real-time plug-in for the working musician, *Proc. Int. Cong. on Acous. (ICA 2016)*, Buenos Aires, Argentina, September, (2016).